Asian Journal of Andrology (2014) 16, 305–308

www.asiaandro.com; www.ajandrology.com

Open Access

ORIGINAL ARTICLE

Prostate Disease

Tissue elasticity displayed by elastography and its correlation with the characteristics of collagen type I and type III in prostatic stroma

Jie Tang[1], Yan Zhang[1], Ming-Bo Zhang[1], Yan-Mi Li[1], Xiang Fei[1], Zhi-Gang Song[2]

We investigated the prostate elasticity displayed by elastography and its correlation with the content and distribution of collagen type I (Col1) and type III (Col3). A total of 62 patients underwent transrectal real-time tissue elastography (TRTE) examinations. Targeted biopsies were performed after 12-core systematic biopsy. The tissues corresponding to the elastograms were stained with picric acid-sirius red. The distribution of Col1 and type Col3 was observed, and the collagen volume fraction (CVF) of these two types of collagen fibers was calculated. The CVFs of Col1 in the stiff and soft groups were 0.05 ± 0.02 and 0.02 ± 0.01 ($P = 0.002$), respectively. The CVFs of Col3 in the stiff and soft groups were 0.05 ± 0.04 and 0.07 ± 0.03 ($P = 0.13$), respectively. The circular analysis results showed that collagen fibers were disorganized both in the soft and stiff groups. Col1 and Col3 were mainly cross-linked, and some parallelization was observed in the sections. The distributions of Col1 and Col3 were different between the stiff and soft groups ($P = 0.03$). In conclusion, the texture of the prostate is due to the content of Col1 and its relative correlation with Col3.
Asian Journal of Andrology (2014) **16**, 305–308; doi: 10.4103/1008-682X.122582; published online: 20 January 2014

Keywords: elastography; extracellular matrix; lesion; prostate; ultrasound

INTRODUCTION

Prostate cancer (PCa) is a common cancer in men and is the second leading cause of cancer-specific death in the Western world.[1] Previous studies have shown that prostate-specific antigen (PSA) testing, transrectal ultrasonography (TRUS), magnetic resonance imaging and TRUS-guided biopsies are useful in the early detection of PCa,[2,3] but 10%–15% of cases of early stage PCa were still missed.[4,5] Tissue elasticity is a biomarker of cancer.[6] Imaging the elastic properties of biological tissues has become a popular topic in much recent research. Transrectal real-time tissue elastography (TRTE) is a new imaging technique that allows for noninvasive estimation and imaging of tissue elasticity distribution within tissues, using conventional real-time ultrasound equipment and modified software. TRTE has been reported to be useful for the differentiation and characterization of PCa,[7-10] with a diagnostic accuracy of 84.1%–91%.[11,12] However, it is unclear why prostate tissue demonstrates stiffness or softness. In previous reports, Pallwein *et al.*[10] expressed the opinion that an increase in cancer cell density results in tissue stiffness. In actual clinical diagnosis, there is some overlap between benign and malignant lesions. Some benign lesions show stiffness on elastography, while some malignant lesions manifest softness on elastography. There have still been no comparative studies on stain imaging and histopathology of the same region. The prostate structure primarily includes two components: gland and stroma. Therefore, do changes in certain components or in the structure of stroma affect tissue texture? Collagen fibers are the major structural extracellular matrix component in the prostate. Collagen type I (Col1) and type III (Col3) are the principal components of normal prostate stroma,[13] while collagen type IV exists mainly in the basement membrane.[14] Therefore, in this study, Col1 and Col3, stained with picric acid-sirius red, were observed, and their correlations with the strain images, displayed by elastography, were investigated.

MATERIALS AND METHODS

Patients

Between December 2009 and February 2010, a total of 62 patients with suspected PCa lesions underwent prostate biopsies. These men were scheduled for prostate biopsies because of serum PSA level (>4 ng ml^{-1}), palpable nodular lesions in digital rectal examination, hypoechoic lesions on TRUS or abnormal magnetic resonance imaging findings (low-intensity lesions on T2-weighted images). Their ages ranged from 52- to 84-years-old (66.6 ± 9.0 years). All of the patients underwent TRTE examinations and prostate biopsy. This study was approved by our local ethics committee. Before biopsy, the risks and benefits of the biopsy procedure were explained to each patient, and written informed consent was obtained from every patient at enrolment. The exclusion criteria were active urinary tract infections, preoperative endocrine treatment[9] or previous transurethral surgery.

Imaging technique

The equipment used was the HI VISION 900 ultrasound system (Hitachi Medical, Tokyo, Japan), which performs real-time tissue elastography. The probe was the EUP-V53W, with a frequency of 4–9 MHz.

All of the patients were scanned in the left decubitus position, with the buttocks located at the edge of the examination bed and the

[1]Department of Ultrasound and [2]Department of Pathology, Chinese People's Liberation Army General Hospital, Beijing, China.
Correspondence: Dr. J Tang (txiner@vip.sina.com)
Received: 02 April 2013; Revised: 05 June 2013; Accepted: 08 August 2013

knees bent toward the chest. Firstly, the prostate was examined by TRUS. Once the lesions were detected, their position, size, boundaries and internal echoes were recorded. Secondly, the real-time tissue elastography mode was switched on, and the elastogram was shown on the monitor, together with the grey-scale ultrasound images. Generally, the elastography sampling box was set sufficiently large to encompass the entire prostate.

TRTE was performed by slight compression and decompression of the prostate, which was induced manually by an experienced physician with at least 8 months of special training, who could ensure the reproducibility. The probe movement was repeated using different compression ratios. The applied force was adjusted according to a visual indicator, which was used to decrease the interobserver variability for TRTE until a stable and reproducible image series was captured. In this study, the optimal strain index displayed on the screen of the visual indicator was 3. The TRTE images were obtained transversely from the base to the apex of the prostate in sequence, and they were recorded on the internal hard disk of the ultrasound equipment. The stiffness of the lesion was displayed from red (soft) to green (intermediate) and blue (hard). The color-coding was standardized, and the same color display was used for all of the patients.

Based on the criteria proposed by König *et al.*[11] blue-colored areas, which had a diameter of at least 5 mm and which were reproducible (after tilting of the US probe) on the elastogram, were regarded as stiff regions. TRTE-targeted biopsy, toward the stiff regions and/or soft regions of the prostate's peripheral zone, was performed transrectally on each patient using an 18-gauge biopsy needle (Biopty; Bard, Covington, GA, USA), powered by an automatic biopsy device. The resulting biopsy specimens were located, marked and fixed in 10% formaldehyde at room temperature. Then, the tissues were embedded in paraffin and sectioned at 4 μm of thickness. Two sections obtained from every specimen were stained with hematoxylin and eosin and picric acid-sirius red, respectively.

The images were visualized with a polarized microscope (6000B, LEICA DM, Wetzlar, Germany) with an Image Acquisition Card (LAS V4.0). The specimens stained with hematoxylin and eosin were analyzed by a specialized prostate pathologist with 20 years of experience. The tissue sections stained with picric acid-sirius red were observed at ×200 magnification, and the collagen fibers in the prostate were located. Six views of each section were randomly selected according to an 'S' shape. The distributions of Col1 and Col3 were observed by two reviewers, who were blinded to patient identity, final diagnosis and the results of other imaging tests. The reviewers acted independently. Agreement between the reviewers was assessed by multirater κ statistics.

Pathology analysis

To quantify the collagen fiber orientation, we used a novel analytic protocol for automatic angle recognition, followed by circular statistics. Automatic angle recognition was achieved using Continuity software (version 6.3b, http://www.continuity.ucsd.edu/Continuity). The fiber angle calculation function in this software was used, based on an intensity gradient algorithm. Continuity software automatically divided an image with dimensions of 640 × 480 pixels into small grids of 20 × 20 pixels in size, and it then calculated the average angle of all the fiber vectors inside the grid. Then, these data were imported into NCSS 2007 (Number Cruncher Statistical Systems, Kaysville, UT, USA) for circular data analysis (see Statistical analysis).

All of the image analyses were performed in a blind manner, using Image Pro Plus (version 6.0, Media Cybernatics, US). The collagen volume fractions (CVFs) of Col1 and Col3 were calculated. The CVF was defined as the sum of stained interstitial collagen tissue areas divided by the entire tissue area.

Statistical analysis

The noncircular data were analyzed using the SPSS (Statistical Package for Social Sciences) software package, version 11.5 for Windows. The quantitative data that obeyed normal distribution and had equal variance were analyzed by *t*-test. The relationships between Col1 and Col3 in the stiff and soft groups were analyzed by the χ^2 test. Receiver operating characteristic curves were used to assess the diagnostic value of collagen fibers. For circular data, only the images were used with angular data that passed the von Mises distribution test. Using descriptive circular analysis, three groups of variables were generated: (i) the circular data's dispersion tendency (circular variance, circular standard deviation (SD) and circular dispersion); (ii) their concentration tendency (mean resultant length and von Wiese concentration (K)); and (iii) the skewness and kurtosis of the circular data. Statistical comparisons of the differences were performed by unpaired *t*-test. $P < 0.05$ were considered statistically significant.

RESULTS

Collagen volume fraction of collagen type I and collagen type III in prostate tissue and the corresponding elastographic findings

Thirty-two of 62 patients had benign prostatic hyperplasia. The remaining 30 cases had PCa, with Gleason scores ranging from 6 to 9.

Among the 62 patients, 35 cases showed stiffness by TRTE examination (**Figure 1** and **2**) and 27 showed softness (**Figure 3**). The CVF of Col1 was 0.05 ± 0.02 in the stiff group and 0.02 ± 0.01 in the soft group. There was a significant difference in the CVF of Col1 between the stiff and soft groups ($P = 0.002$). The area under the receiver operating characteristic curve of the CVF of Col1, in differentiating stiff tissue from soft tissue, was 0.88 ($P = 0.003$). At the cutoff value of 0.03, the CVF of Col1 yielded the highest sensitivity (88.9%) and specificity (87.5%).

Circular analysis of the collagen fibers in prostate lesions

Various appearances (network, compact, loose and fuzzy and so on) of the collagen fibers were observed in the prostate lesions (**Figure 1b, 2b** and **3b**). The quantitative analysis results showed that all the Col1 and Col3 were disorganized in both the soft and stiff groups. There was no difference between the soft and stiff groups in the parameters of circular analysis (circular variance, circular SD and circular dispersion; mean resultant length and von Wiese concentration; skewness and kurtosis) ($P > 0.05$) (see the box-whiskers plot in **Figure 4**).

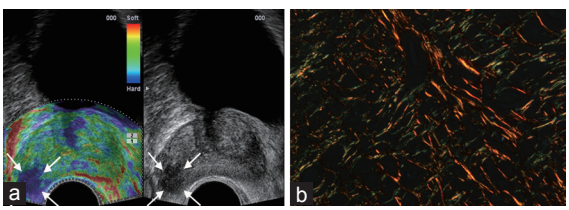

Figure 1: Elastography of prostate cancer (stiff lesion). (**a**) A hypoechoic lesion without a clear boundary was found in the right peripheral zone of the prostate by TRUS (right image, white arrow), and a local blue region indicated the lesion by TRTE (left image, white arrow). (**b**) The section stained with picric acid-sirius red showed that Col1 and Col3 were cross-linked in distribution. The collagen volume fraction of Col1 (0.05) was greater than that of Col3 (0.02). TRTE: transrectal real-time tissue elastography; TRUS: transrectal ultrasonography.

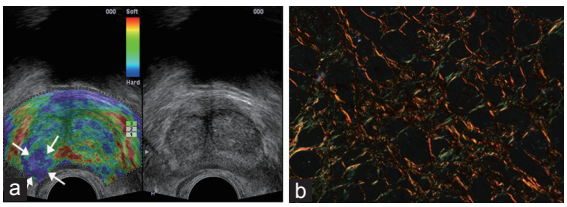

Figure 2: Elastography of benign prostatic hyperplasia (stiff lesion). (**a**) No obvious lesion was found in the peripheral zone of the prostate by TRUS (right image), but a local blue area appeared in the right peripheral zone of the prostate by TRTE (left image, white arrow). (**b**) The section stained with picric acid-sirius red showed that Col1 and Col3 were cross-linked in distribution. The collagen volume fraction of Col1 (0.04) was greater than that of Col3 (0.01). TRTE: transrectal real-time tissue elastography; TRUS: transrectal ultrasonography.

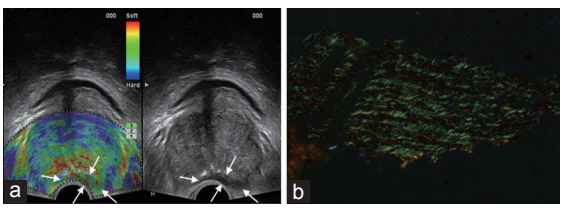

Figure 3: Elastography of prostate cancer (soft lesion). (**a**) A hypoechoic lesion without a clear boundary was found in the peripheral zone of the prostate by TRUS (right image, white arrow). The main body of the lesion was shown as green and red by TRTE (left image, white arrow). (**b**) The section stained with picric acid-sirius red showed that Col1 and Col3 were not cross-linked in distribution. The collagen volume fraction of Col3 (0.6) was greater than that of Col1 (0.02). TRTE: transrectal real-time tissue elastography; TRUS: transrectal ultrasonography.

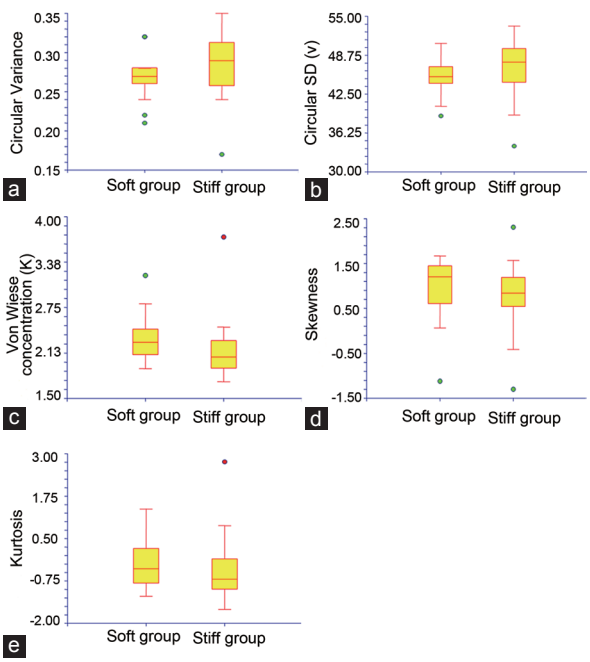

Figure 4: Box-whiskers plot of collagen fibers. (**a–e**) Comparisons of parameters derived from circular statistics of collagen fibers. The boxes extend from 25 to 75%, with a line at the median. There was no difference between the soft and stiff groups in the parameters of circular analysis (circular variance, circular standard deviation, and circular dispersion; mean resultant length and von Wiese concentration; skewness and kurtosis) ($P > 0.05$).

The elastographic findings and the relationship between collagen type I and collagen type III

Col1 and Col3 were mainly cross-linked or in parallel distribution, as observed in the sections. The two reviewers showed good agreement in assessing the relationship between Col1 and Col3, and the κ value was 0.81.

Thirty-two of 35 patients (91.43%) in stiff group showed Col1 and Col3 in cross-linked distribution and three cases showed parallel distribution. Nineteen of 27 (70.37%) patients in the soft group showed Col1 and Col3 that were cross-linked and eight cases were not cross-linked, of which seven cases were in parallel distribution. The distributions of Col1 and Col3 were different between the stiff and soft groups ($\chi^2 = 4.63$, $P = 0.03$).

DISCUSSION

Previous studies have shown that the stroma plays an important role in the growth and differentiation of the normal prostate, and it also has a close relationship with the occurrence of benign prostatic hyperplasia and PCa.[15] Collagen fibers, the major structural components of the extracellular matrix, change in arrangement and integrity with increasing age.[16] The network of fibers varies in normal and diseased states. In benign prostatic hyperplasia, the collagen network is dense, with a large number of fibers. In prostatic adenocarcinoma, there is nonuniform swelling, with a loss and disintegration of collagen fibers.[17] Collagen fibers are a stiff biomaterial with a small strain. Under a normal range of force, its strain range is 6%–8%, and when the external force is sufficiently great to break the collagen fibers, the strain only increases by 4%–7%.[18]

This study investigated the correlation between collagen fibers (I, III) and the corresponding elastography. The quantitative analysis of collagen fibers showed that the CVF of Col1 in the stiff group was greater than that in the soft group ($P < 0.05$). However, the CVF of Col3 had no significant difference between the stiff and soft groups ($P > 0.05$). This result suggests that the Col1 content was related to tissue texture. Previous studies have also reported that high Col1 fiber content corresponds to more rigid and less compressible tissue properties.[13,19]

Regarding the shape of collagen fibers, Col1 was thick, but Col3 was very thin. Furthermore, the arrangement of collagen fibers was dense where the area was rich in Col1, but the arrangement of collagen fibers was thin where the area was rich in Col3.[20] Continuity software has been used widely in the collagen fiber analysis for automatic angular recognition.[21] The results of this study showed that the collagen fibers angles were not different between the stiff and soft groups by quantitative analysis. However, further observation of the relationship between Col1 and Col3 showed that parallel relationships were seldom seen in these sections, and they existed mainly in the soft group. The cross-linked style of Col1 and Col3 was common and was mainly found in the stiff group ($P < 0.05$). Cross-link formation is a critical step in the maturation of collagen fibers to provide tensile strength. [13] The cross-linked relationship of Col1 and Col3 strengthened the cross-linking of total collagen fibers, which rendered the tissue stiffer. As shown in the previous literature, the collagen cross-linking of collagen fibers was confirmed to increase mechanical strength,[22,23] and the inhibition of the cross-linking procedure resulted in reduced tissue stiffness.[24] This method has been applied in the treatment of keratoconus, intractable corneal ulcerations, keratitis and so on. As mentioned above, the content of Col1 and the distribution of Col1 and Col3 were related to the elastography of the prostate. However, there were three cases in which Col1 and Col3 ran in parallel directions in the stiff group, and their CVFs of Col1 were 0.05, 0.03 and 0.04,

respectively, namely, greater than or equal to 0.03. However, in the soft group, there were 19 cases in which the relationship of Col1 and Col3 was cross-linked distribution, and only six cases had CVFs of Col1 greater than 0.03. These results indicated that the tissue stiffness was dependent firstly on the content of Col1 and secondly on the distribution between Col1 and Col3.

This study helped us to understand some reasons why strain images show stiffness or softness, and the results are encouraging for future clinical diagnosis. However, the study still had some limitations. Although we gained some experience in the diagnosis of PCa using TRTE in previous studies, and we have reported a method for decreasing and identifying the artefacts of images, the manual compression method can still cause some misinterpretation of stiffness, and relative stiffness measurements cannot reflect the specific stiffness degrees between lesions from different subjects. The application of novel equipment, such as real-time balloon inflation elastography,[25] and of absolute tissue stiffness measurement approaches (such as supersonic shear wave imaging and acoustic radiation force imaging) will be more powerful in reflecting the real tissue texture. In addition, samples obtained from biopsy cannot reflect the information in tissue completely, and other factors that might affect tissue stiffness will be investigated in future studies.

AUTHOR CONTRIBUTIONS

JT conceived of this study, participated in the acquisition of data, and drafted the manuscript. YZ and MBZ performed the statistical analysis and interpreted the data. YML and XF helped to draft the manuscript. ZGS performed the pathological analysis. All authors read and approved the final manuscript.

COMPETING INTERESTS

All authors have no competing financial interests.

ACKNOWLEDGMENTS

Financial support from the National Natural Science Foundation (81071279, 8100019) and the National Technology Support Plan (2009BAI 86B05) is gratefully acknowledged. We are grateful to be licensed for the use of Continuity 6.3b software from National Biomedical Computation Resources (National Institutes of Health Grant P41-RR-08605), Cardiac Mechanics Research Group, University of California, San Diego, USA.

REFERENCES

1 Gu F. Epidemiological survey of benign prostatic hyperplasia and prostate cancer in China. *Chin Med J* (*Engl*) 2000; 113: 299–302.
2 Borley N, Feneley MR. Prostate cancer: diagnosis and staging. *Asian J Androl* 2009; 11: 74–80.
3 Catalona WJ Richie JP Ahman FR, Hudson MA, Scardino PT, *et al*. Comparison of digital rectal examination and serum prostate specific antigen in the early detection of prostate cancer: results of a multicenter clinical trial of 6630 men. *J Urol* 1994; 151: 1283–90.
4 Halpern EJ, Frauscher F, Rosenberg M, Gomella LG. Directed biopsy during contrast-enhanced sonography of the prostate. *AJR Am J Roentgenol* 2002; 178: 915–9.
5 Norberg M, Egevad L, Holmberg L, Sparén P, Norlén BJ, *et al*. The sextant protocol for ultrasound-guided core biopsies of the prostate underestimates the presence of cancer. *Urology* 1997; 50: 562–6.
6 Hoyt K, Castaneda B, Zhang M, Nigwekar P, di Sant'agnese PA, *et al*. Tissue elasticity properties as biomarkers for prostate cancer. *Cancer Biomark* 2008; 4: 213–25.
7 Aigner F, Pallwein L, Junker D, Schäfer G, Mikuz G, *et al*. Value of real-time elastography Targeted biopsy for prostate cancer detection in men with prostate specific antigen 1.25 ng/ml or greater and 4.00 ng/ml or less. *J Urol* 2010; 184: 913–7.
8 Zhang Y, Tang J, Li YM, Fei X, He EH, *et al*. The contribution of strain patterns in characterization of prostate peripheral zone lesions at transrectal ultrasonography. *Acta Radiologica* 2012; 53: 119–26.
9 Miyanaga N, Akaza H, Yamakawa M. Tissue elasticity imaging for diagnosis of prostate cancer: a preliminary report. *Int J Urol* 2006; 13: 1514–8.
10 Pallwein L, Mitterberger M, Struve P, Horninger W, Aigner F, *et al*. Comparison of sonoelastography guided biopsy with systematic biopsy: impact on prostate cancer detection. *Eur Radiol* 2007; 17: 2278–85.
11 König K, Scheipers U, Pesavento A, Lorenz A, Ermert H, *et al*. Initial experiences with real-time elastography guided biopsies of the prostate. *J Urol* 2005; 174: 115–7.
12 Pallwein L, Mitterberger M, Struve P, Pinggera G, Horninger W, *et al*. Real-time elastography for detecting prostate cancer: preliminary experience. *BJU Int* 2007; 100: 42–6.
13 Shoulders MD, Raines RT. Collagen structure and stability. *Annu Rev Biochem* 2009; 78: 929–58.
14 Isisag A, Nese N, Ermete M, Lekili M, Ayhan S, *et al*. Col IV and Fn distribution in prostatic adenocarcinoma and correlation of 67LR, MMP–9 and TIMP–1 expression with Gleason score. *Anal Quant Cytol Histol* 2003; 25: 263–72.
15 Zhang Y, Nojima S, Nakayama H, Jin Y, Enza H. Characteristics of normal stromal components and their correlation with cancer occurrence in human prostate. *Oncol Rep* 2003; 10: 207–11.
16 Bianchi-Frias D, Vakar-Lopez F, Coleman IM, Plymate SR, Reed MJ, *et al*. The effects of aging on the molecular and cellular composition of the prostate microenvironment. *PLoS ONE* 2010; 5: 1–16.
17 Morrison C, Thornhill J, Gaffney E. The connective tissue framework in the normal prostate, BPH and prostate cancer: analysis by scanning electron microscopy after cellular digestion. *Urol Res* 2000; 28: 304–7.
18 Kai ZT, Er YC, Guang RD. Structure and biomechanics of collagen fibers. *Prog Anat Sci* 1998; 4: 289–93.
19 Wenger MP, Bozec L, Horton MA, Mesquida P. Mechanical properties of collagen fibrils. *Biophys J* 2007; 93: 1255–63.
20 Zhi YH, Hong WC, Ning W. Immunohistochemical study of the extracellular matrix of prostate cancer. *Tumor* 1995; 15: 96–7.
21 Zhou X, Yun JL, Han ZQ, Gao F, Li H, *et al*. Postinfarction healing dynamics in the mechanically unloaded rat left ventricle. *Am J Physiol Heart Circ Physiol* 2011; 300: H1863–74.
22 Chai D, Gaster RN, Roizenblatt R, Juhasz T, Brown DJ, *et al*. Quantitative assessment of UVA-riboflavin corneal cross-linking using nonlinear optical microscopy. *Invest Ophthalmol Vis Sci* 2011; 52: 4231–8.
23 Wollensak G, Spörl E, Seiler T. Treatment of keratoconus by collagen cross linking. *Ophthalmologe* 2003; 100: 44–9.
24 Bruel A, Ortoft G, Oxlund H. Inhibition of cross-links in collagen is associated with reduced stiffness of the aorta in young rats. *Atherosclerosis* 1998; 140: 135–45.
25 Tsutsumi M, Miyagawa T, Matsumura T, Endo T, Kandori S, *et al*. Real-time balloon inflation elastography for prostate cancer detection and initial evaluation of clinicopathologic analysis. *AJR Am J Roentgenol 2010*; 194: W471–6.

How to cite this article: Tang J, Zhang Y, Zhang MB, Li YM, Fei X, Song ZG. Tissue elasticity displayed by elastography and its correlation with the characteristics of collagen type I and type III in prostatic stroma. *Asian J Androl* 20 January 2014. 10.4103/1008-682X.122582. [Epub ahead of print]